https://doi.org/10.5194/egusphere-2025-2623
Preprint. Discussion started: 2 October 2025

Using Cave Drip Loggers to Characterize Groundwater Infiltration and Examine Hydrological Response in Cretaceous Karst Formation

Rowann Remie[1], Kashif Mahmud[1], Marcus Gary[2], Jonathan D. Price[1], Andrew Katumwehe[3], and Brian Vauter[4]

1Kimbell School of Geoscience, Midwestern State University, Wichita Falls, TX 76308
2Jackson School of Geosciences, University of Texas, Austin, TX 78712
3Boone Pickens School of Geology, Oklahoma State University, Stillwater, OK 74078
4Natural Bridge Caverns, 26495 Natural Bridge Caverns Road, San Antonio, TX 78266

Correspondence to: Kashif Mahmud (kashif.mahmud@msutexas.edu) and Rowann Remie (rnremie2@gmail.com)

Abstract. In Texas, groundwater from karst aquifers represents a significant percentage of the State's water supply. Karst regions are vital groundwater resources, and caves offer natural access points for observing long-term vadose zone water storage and fluxes, offering a better understanding of groundwater flow paths. Natural Bridge Caverns (NBC), which is situated within the recharge zone of the Cretaceous age Edwards (Balcones Fault Zone) aquifer and also recharges the Trinity aquifer below the Edwards, was monitored with a high resolution, spatially dense cave drip rate network during one hydrological year to characterize water infiltration within this karst system. Precipitation, soil water content (SWC) and evapotranspiration (ET) data were obtained for the location and used to evaluate infiltration-discharge relationship for 20 drip loggers. All drip sites remained active throughout the monitoring period, and generally exhibited low discharge rates during dry periods and high discharge rates in response to rainfall events. Discharge at the drip sites varied substantially, and analysis revealed a spatial relationship emerging from the dataset. Using Multidimensional Scaling (MDS) and agglomerative hierarchical clustering (AHC) we were able to classify similar drip types to obtain four unique drip regimes. A lithological assessment suggests that secondary porosity is influencing water movement rather than overburden thickness. Despite the relatively short time frame of this study, we find that the results shed valuable insights into the heterogeneity of hydrological flow within the vadose zone at NBC. It also emphasizes the importance of advancing our understanding and characterization of unsaturated zone hydrological processes to inform effective groundwater management policies.

1 Introduction

Groundwater is the largest source of freshwater globally. It supports a wide range of critical ecosystems and is also used for a myriad of human activities (Rohde et al., 2024). Groundwater plays a crucial role in adapting to climate change impacts. Climate resilience for water supplies is frequently linked with a transition towards increased reliance on groundwater, therefore

https://doi.org/10.5194/egusphere-2025-2623
Preprint. Discussion started: 2 October 2025

protecting primary infiltration and recharge areas would be of significant benefit (Stigter et al., 2022). Dependence on groundwater is expected to increase in the future as the availability of surface water becomes limited due to drought, contamination, and climatic variability, making groundwater a possible solution for future 'water crisis' (Li et al., 2017). Therefore, improving the management of groundwater as a resource is critical to understand its availability at a time when climate is becoming increasingly unpredictable. Several groundwater studies suggest that large portions of karst aquifers in the northern hemisphere temperate zone could be severely impacted in the future by diminished recharge as a result of climate change (Goldscheider et al., 2020). Possible negative impacts of climate change on groundwater recharge include altering temperature and evaporation rates, as well as rainfall amounts, intensity, and runoff (Nielsen-Gammon et al., 2020).

Karst carbonate terrains cover approximately 15.2 % of the Earth's land surface (Goldscheider et al., 2020; Chapman et al., 2024), with groundwater from karst aquifers supplying about 9.2 % of the global population worldwide (Stevanović, 2019; Chapman et al., 2024). In Texas, groundwater is a vital water source, with local aquifers supplying approximately 60 % of total water used (Texas Water Development Board, 2020). The state's groundwater is sourced from 31 aquifers, with nine major aquifers holding about 97 percent of the available groundwater (Texas Comptroller of Public Accounts, 2022). This vast volume underscores the importance of managing groundwater resources sustainably, especially as the state anticipates a population growth of 73 % between 2020 and 2070, from 29.7 million to 51.5 million, along with a projected 9 % increase in water usage. Current water supplies for drought conditions are also expected to decline by approximately 18 % for that same time period, primarily as a result of aquifer depletion and climate variability. The anticipated demand for groundwater resources, underlies current conservation efforts and to inform proper management practices (Texas Water Development Board, 2022). The south-central Texas region relies primarily on karst-groundwater systems for personal, commercial, and industrial use; therefore, it is of great importance to understand this valuable asset for sustainable use. Karst aquifers are particularly vulnerable to contamination due to their heterogeneous nature and overall connectivity of flow pathways that accelerate contaminant migration (Ford and Williams, 2013; Chapman et al., 2024). In order to properly manage this resource, we need to better comprehend water infiltration flow paths through limestone in karst terrains (Mahmud et al., 2016; Baker et al., 2020; 2021).

Karst regions consist of three distinct horizons, the epikarst (subcutaneous) zone, vadose (infiltration) zone, and phreatic (saturated) zone, each exhibiting varying degrees of porosity and permeability (Williams, 1983; Bauer et al., 2005). The uppermost layer, the epikarst, is recognized as a substantial water reservoir with higher porosity and permeability compared to the underlying vadose zone and includes any soil horizons that may exist. (Klimchouk, 2004; Markowska et al., 2015). Karst limestone regions contain conduits that facilitate water storage and flux within the epikarst and typically exhibit elevated infiltration rates through fractures and bedding planes, the predominant recharge mechanism for unconfined aquifers (Ford and Williams, 2013; Mahmud et al., 2018; Chapman et al., 2024). In karst environments, infiltrating water moves from the unsaturated zone to the water table, but flow can be delayed to varying degrees depending on changes in surface conditions. As a result, recharge may occur almost instantaneously (Wong et al., 2011; Nielsen-Gammon et al., 2020), or it may take hundreds or even thousands of years, as suggested by radiocarbon dating (McMahon et al., 2011). This water seepage is

https://doi.org/10.5194/egusphere-2025-2623
Preprint. Discussion started: 2 October 2025

controlled by different porosity types within the soil or rock material, which govern the movement and flow of water and creates distinct infiltration pathways (Markowska et al., 2015).

Speleogenesis, the process by which accumulated surface water is leached through fracture porosity in karst terrain, contributes to the dissolution of the underlying soluble rock, eventually leading to the formation of void-conduit systems or cavernous porosity (caves) (Klimchouk, 2015). In epigenic karst systems, this process primarily occurs within the epikarst (Chapman et al., 2024), where the combination of increased porosity and permeability allows for enhanced water infiltration that can enlarge fractures and bedding planes, increasing the pathways for groundwater flow. The heterogeneity of these flow paths enables meteoric water to infiltrate from the vadose zone through extensive fracture systems, with preferential percolation flow routes emerging as drip waters within caves (Jex et al., 2012), from ceiling speleothems (stalactites). These formations develop due to the deposition of calcium carbonate (calcite) that precipitates from water percolating through the carbonate rock. Karst systems are marked by significant subsurface variability and their intricate recharge processes are difficult to define and characterize. The heterogeneous nature of karst leads to a non-linear response to surface precipitation and cave discharge, which are key mechanisms for groundwater recharge (Baker and Brunsdon, 2003; Markowska et al., 2015). Rainfall events provide valuable insight into subsurface water movement, with the transport of vadose water through cave systems playing an essential role in replenishing groundwater supplies to local aquifers (Baker et al., 2021). The cavernous porosity typical of karst landscapes, therefore, provides an ideal environment in which to study the infiltration of vadose-zone water.

Previous attempts have sought to develop conceptual cave drip water hydrology models that classify drip rate variations according to their response to recharge events such as Smart and Friederich (1987), who noted a range of discharge volumes and variabilities from almost unvarying low volumes, from consistently low seepages to highly variable flows that quickly respond to recharge. Their results were eventually used to develop a hydrological classification model for flow rate changes within unsaturated zones (Tooth and Fairchild, 2003; McDonald and Drysdale, 2007; Jex et al., 2012) and to illustrate the relationships between interconnectivity and flow path (Markowska et al., 2015). The characterization of drip hydrology was later modified by Baker et al. (1997) and Baldini et al. (2006), whose studies enhanced the understanding of how drip waters respond to varying environmental conditions, such as rainfall events, temperature, temporal changes, and seasonal fluctuations. Hydrological parameters that exhibit some control on flow rate include rainfall, groundwater flow, evapotranspiration (ET) and soil water content (SWC), which serve as inputs that promote recharge (Mariethoz et al., 2012). Additionally, Chapman et al. (2024), examined ET along with bedrock depth and overburden in the vadose zone. Nava-Fernandez et al. (2020) and Baker et al. (2021) also explored drip water and the relationship between atmospheric conditions while Jex et al. (2012) and Mahmud et al. (2018), examined automatic drip logging to obtain insight into subsurface interactions and model recharge rates, both of whom proposed a classification system based on drip discharge time series, statistical testing, and clustering models. These previous research projects have provided a foundational understanding of cave drip hydrology and its impact on karst systems and laid the groundwork for this current study, for example Baker et al. (2020) defined groundwater recharge as the "downward flow of water reaching the water table, adding to groundwater storage." Diffuse recharge is precipitation-driven infiltration through the unsaturated zone across significant areas of the landscape. This process occurs beneath the zero-flux

https://doi.org/10.5194/egusphere-2025-2623
Preprint. Discussion started: 2 October 2025

plane (ZFP), which separates the zones of upward and downward moving waters (Baker et al., 2020; 2021). The ZFP is typically assumed to be at the depth of the vadose zone, where the flux of water moving downward is balanced by the upward movement of water due to evaporation and capillary rise. Additionally, diffuse recharge is a critical process for replenishing groundwater supplies, especially in areas where direct infiltration from rainfall is significant. Rainfall recharge threshold is defined as the precipitation condition required to overcome a combination of evapotranspiration losses and soil moisture deficits (Baker et al., 2020; 2021) and trigger water infiltration into the subsurface to replenish aquifers below.

Rainfall and SWC are fundamental drivers of groundwater recharge. Rainfall constitutes a primary source of direct recharge, with its magnitude, intensity, and duration acting as principal controls (Yinglan et al., 2018). These factors are further mitigated by surface properties, including soil cover, vegetation density, and substrate permeability. Seasonal variations in rainfall significantly influence groundwater recharge rates and infiltration dynamics, making them critical components in accurately simulating hydrological processes (Yinglan et al., 2018). These temporal changes affect the timing and magnitude of water percolation through the soil profile, thereby impacting subsurface storage, runoff generation, and overall watershed response. SWC represents the amount of water retained within the soil matrix at a given time, reflecting the balance between water inputs from precipitation and losses due to drainage and evapotranspiration. High SWC enhances the potential for groundwater recharge, as more water is available to infiltrate. Increased rainfall frequency can elevate SWC, leading to more significant groundwater recharge, whereas low-frequency rainfall can lower SWC, trapping water at the surface (Wu et al., 2023).

To measure infiltration, commercially-available automatic acoustic drip rate loggers, (e.g., Mahmud et al., 2018)., offer reliable and cost-effective time-series data collection (i.e., drips per time). Assuming a constant drip volume, the logger provides infiltration data for individual speleothems. Strategic placement of loggers profiles the overall pattern for the cavern overburden. For this study, cave-water infiltration was evaluated with respect to rainfall, SWC, observed flow patterns, host lithology, and overburden thickness to understand water infiltration pathways and gain insights into subsurface interactions on site.

2 Site Description

2.1 Geologic Background

The strata of the study area primarily consist of Early Cretaceous limestone, marl, and shale from the Trinity and Edwards Groups. These layers represent more than 600 m (2000 ft.) of shallow marine, shelf margin deposits (Collins, 1998). The formations in each group serve as host strata for groundwater largely through enhanced-fracture systems. The principal hydrologic units in this region are the Glen Rose Formation (Trinity Group) and the Kainer and Person Formations (Edwards Group); the latter is overlain by the Georgetown Formation and confined by the Del Rio Clay of the Washita Group (Schindel and Gary, 2017). The Glen Rose Formation is a marine fossiliferous limestone and dolostone interbedded with shale, clay, and marl with layers of gypsum and anhydrite (Schindel, 2019); evaporites are a prominent feature at the base of the upper member. The Kainer and Person Formations are characterized by high-frequency depositional cycles, including various subtidal

https://doi.org/10.5194/egusphere-2025-2623
Preprint. Discussion started: 2 October 2025

carbonate rocks (Collins and Hovorka, 1997). Lithologic units consist of argillaceous carbonate rocks at the base and middle, and argillaceous tidal-flat mudstone and evaporite in the Person (Pantea and Cole 2004). Locally, the basal Kainer Fm. is nodular, pelloidal and burrowed mudstone to grainstone.

All are offset by the Balcones Fault Zone (BFZ), a system of high-angle normal faults down-thrown towards the Gulf of Mexico that formed during the middle to late Tertiary (Ferrill et al., 2004). The Neogene faulting follows the subsurface axis of the Pennsylvanian Ouachita Fold Belt, and faults appear to extend into and displace the rocks of the underlying structural belt (Maclay and Small, 1986). The Texas Water Development Board recognizes a separate major aquifer for the faulted expression, the Edwards Aquifer BFZ, where structural control transitions the aquifer from unconfined (i.e., exposed Edwards Group) to confined (i.e., overlain by Del Rio Clay).

2.2 Hydrologic Background

The formation of a karst aquifer system within the Edwards is attributed to two significant events. The penecontemporaneous (Late Albian) uplift of the San Marcos Platform resulted in local erosion, dissolution by meteoric water, and karst formation (Barker et al., 1994). Subsequent Miocene and younger Edwards Plateau uplift along the BFZ produced more than 300 m (1000 ft.) of displacement (Collins, 1998). The uplifted Edwards Group was stripped of overburden and exposed to increasing meteoric-water circulation, which leached out significant volumes of evaporite minerals and dolomite (Maclay and Small, 1986; Cole and Pantea, 2004). The structure and evolution of the BFZ strongly influence flow patterns in the Trinity and Edwards Aquifers (Maclay and Small, 1986; Barker et al., 1994). The fault structure affects the hydraulic gradient in the system (Maclay and Small, 1983; Cole and Pantea, 2004). The gross permeability of the aquifers is shaped by BFZ faulting and related deformation, with conduits and solution features propagating along fractures (Hovorka and others, 1995; Collins and Hovorka, 1997). Surface features of the Edwards Limestone include sinkholes, sinking streams, caves, springs, and a subsurface drainage system (Maclay and Land, 1988; Schindel and Gary, 2017).

The Edwards (BFZ) Aquifer has three major sections: the contributing, recharge, and artesian zones. Permeability is largely through faults, joints, fractures, and dissolution-induced networks (Buszka and others, 1990; Maclay and Small, 1986; Small and Hanson, 1994; Schindel and Gary, 2017). The Glen Rose Formation, the uppermost unit of the Trinity Aquifer, generally defines the lower boundary of the aquifer. The degree of hydraulic connection between the Trinity and Edwards (BFZ) Aquifers is locally limited by the relatively low vertical hydraulic conductivities of the basal Edwards and upper Trinity Groups, but on a regional scale, karstic features allow cross-formational flow to occur (Lindgren et al., 2004).

The Edwards (BFZ) Aquifer is one of the most important and prolific karst aquifers in the United States. It is a source of water for more than two million people in the greater San Antonio area and an essential resource for municipal, agricultural, and industrial use within Comal County and surrounding 7 counties (Schindel, 2019). It is also the sole habitat for numerous Federally listed endangered species. The aquifer functions as both a confined and unconfined system, with an outcrop area of 4,030 square km (1,566 square miles) and a total subsurface extent of 6,425 square km (2,481 square miles). Among all Texas aquifers, it discharges the greatest volume of baseflow per square mile of aquifer area (Bruun et al., 2016). The Edwards BFZ

https://doi.org/10.5194/egusphere-2025-2623
Preprint. Discussion started: 2 October 2025

Aquifer is recognized as being highly vulnerable to climate change due to its shallow depth and high karst permeability that allows for rapid surface-subsurface interactions (Wong et al., 2012; Nielsen-Gammon et al., 2020).

2.3 Study Location

Natural Bridge Caverns (NBC), (29.69 N, 98.34 W), is located between New Braunfels and San Antonio in Comal County, Texas (Fig. 1A). It was first discovered in 1960 and eventually developed as a privately-owned commercial cavern that opened to the public in 1964. It is a show cave opened daily with 250,000 annual visitors. Its name is derived from the sixty-foot natural span of limestone that forms a bridge across the large collapsed doline directly behind the visitor center (Kastning, 1983). The caverns are situated within the contributing zone of the Trinity unconfined Aquifer and the recharge area of the Edwards Aquifer (Elliott and Veni, 1994; Heidmann, 1995). The surface above the Caverns is covered with thin (<30 cm) clay-rich mollisols that hosts juniper, oak, savanna grasses, and cacti (Musgrove and Banner, 2004). It has been hypothesized by Schindel and Gary (2017), that many Edwards relict caves were formed by ascending water, associated with paleosprings that were abandoned as the water table deepened. Much of the recharge to these aquifers is attributed to rainfall runoff, which moves across the karst terrain and is eventually lost to faults, fractures, sinkholes, and caves (Collins, 1998).

The roof and upper portions of NBC are in the lower Kainer Formation, but the cave is mainly formed within the upper member of the Glen Rose Formation (Small and Hanson, 1994; Musgrove and Banner, 2004; Cowan et al., 2013). The caverns have a lateral extent of 1160 m and a maximum depth of 75 m (Elliott and Veni, 1994; Wong and Banner, 2010). The Bat Cave Fault is a large, regional break mapped from Cibolo Creek north across Comal County into Hays County. This fault juxtaposes the Kainer Formation with the Glen Rose Formation, observed in the southernmost section of NBC. NBC has two major sections, a southern section named the Hidden Passages and a northern section named the Discovery Passages, which is the focus of this study. NBC's Discovery Passages have 13 defined sections (Gary, 2011) including the Castle of the White Giants and the Exit Tunnel section, which includes the largest room - the Hall of the Mountain King.

The average annual rainfall for the site is 740 mm/year based on records from 1856 to 2008, varying from 250 to 1320 mm/year. The climate regime at the cavern's location is sub-humid to semi-arid (Wong et al., 2011). Evaporation of 1,905 to 2,286 mm (75 to 90 inches) per year removes much of this water prior to infiltration. Rainfall events are typically thermal-convection thunderstorms, which generate large amounts of precipitation in a short timeframe (Gary, 2011). The annual recharge varies in response to regional precipitation, with approximately 85-90% of regional precipitation lost to evapotranspiration (Maclay, 1995; Musgrove and Banner, 2004). According to Kastning (1983), water enters the cave by infiltration even during dry periods, and this seepage promotes the continuous development of speleothems within the cavern.

https://doi.org/10.5194/egusphere-2025-2623
Preprint. Discussion started: 2 October 2025

3 Materials and Methods

3.1 Field investigation

Twenty automatic acoustic drip loggers (Stalagmate® drip loggers Mk3c from www.driptych.com) were installed within NBC's Discovery Passages on 15 May 2023. The drip logger is entirely solid state and fully self-contained in a rugged enclosure approximately 60 by 60 mm (Collister and Mattey, 2005). Each logger was placed on a cloth bean bag to provide stability. The logger uses a piezo-electric response technique for signal detection. It detects individual drops and records the total drop count between a predefined time interval (Collister and Mattey, 2008). It provides a high-resolution record of changing drip rates insensitive to spurious noise, sensing drips sourced from 25 cm or higher. The loggers were configured using the Gemini Tiny Tag software before deployment onsite.

We downloaded data on 13th January 2024 and then on May 19th 2024 for a total of one year of drip time series. Due to the time required to identify each location and complete the installations, data collected on the first day was discarded. Likewise, we discarded all data recorded during the fieldwork hours of subsequent visits. Logger 14 was removed from its position on 16 May, 2024 by the Cavern's staff due to environmental concerns: high water volume at this location leached the dye from the bean bag, staining the stalagmite formation. In order to maintain the same number of counts across the entire 20 datasets, all data was truncated to match the 16 May removal time of logger 14. This left a total of 35,162 15-minute interval entries recorded for each logger. Drip data collection is ongoing, however here we present one hydrological year, covering both wet and dry seasons.

The strategic distribution of the drip loggers covers an elevation gradient to assess the impact of overburden thickness on water infiltration. The selected sites are spatially distributed throughout the two largest chambers (Castle of the White Giants and the Hall of the Mountain King), along with the connecting passageways (Fig. 1B). Multiple sites were identified as actively dripping locations associated with different speleothem formations (Fig. 1D), including chandeliers, stalactites, soda straws, and flowstones. Previous studies (e.g., Genty and Deflandre, 1998) suggest that monitoring at least one hydrological cycle of dripping water is sufficient to observe seasonal variations in karst water movement.

The Castle of the White Giants is formed entirely in the cavernous (upper) member of the Glen Rose Formation (Fig. 1C). It lies on a large mass of breakdown formed from roof collapse, which is now almost completely covered by secondary calcite and is characterized by a vast number of ceiling features and massive speleothems. Large precipitation events have periodically inundated the room (Gary, 2011). The Hall of the Mountain King is the largest chamber section at NBC, formed along a trend similar to regional faulting (azimuth ~060°). The ceiling is highly decorated with cave formations that correspond with abundant dripstone features, many of which have developed on a large floor breakdown pile. This section is formed in the basal nodular member of the Kainer Formation. The connecting passageway between the two sections is part of the water flow that extends beyond the study area. This was formed as water flowing through the cave cut down through the limestone, and it also includes the Emerald Lake section (Gary, 2011).

https://doi.org/10.5194/egusphere-2025-2623
Preprint. Discussion started: 2 October 2025

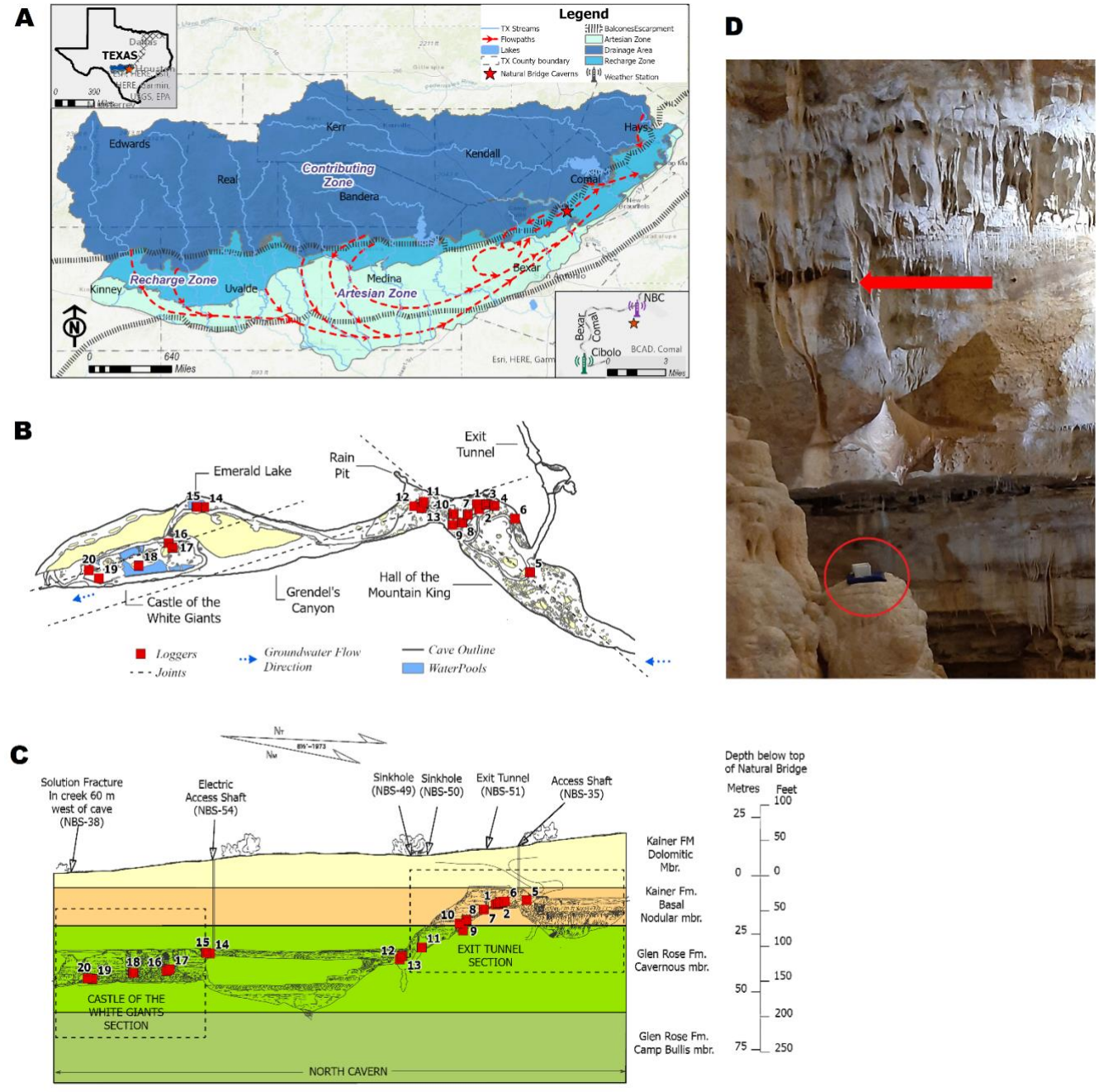

Figure 1: (A) Location of NBC (red star), overlain on a map of the Edwards (BFZ) Aquifer showing Balcones escarpment, water bodies and general groundwater flow pattern (adapted from Collins and Horvoka, 1997). (B) Cropped plan of study area showing approximate distribution of drip loggers (red squares), joints and fractures and groundwater flow direction, adapted from Vauter (2022). (C) Depth Profile with stratigraphic information overlain to highlight the regional geologic units within which the cave is developed as well as approximate logger placement. (Modified from Knox, 1978; Vauter 2000; Gary, 2011). (D) Placement of Logger 13 (highlighted by red circle), supported by a cloth bean bag, beneath dripping ceiling formation (indicated by red arrow).

https://doi.org/10.5194/egusphere-2025-2623
Preprint. Discussion started: 2 October 2025

3.2 Weather data

Daily precipitation and soil water content (SWC) of 10 cm of topsoil were obtained from the Edwards Aquifer Authority (EAA), a HOBO weather station (ID. No. COM04WS) located at NBC (29.69915 N, 98.34196 W). Dataset is available for download from the website at https://www.texmesonet.org, as Natural Bridge Caverns (EAA) | E011. Evapotranspiration (ET) data was provided by EAA from the Cibolo Creek site, approximately 2.5 miles away. This is an eddy covariance station installed at the EAA Field Research Park (FRP) located near Cibolo Creek and referred to in EAA documentation as "Cibolo (US-EA4)". The site is in an oak-ashe-juniper woodland ecosystem. The station operates with a CR1000X datalogger and EasyFlux-DL program. It includes a 4-way radiometer (SN500SS, Apogee), a photosynthetically-active radiation (PAR) sensor (CS310, Apogee), ground-based sensors including one self-calibrating heat-flux plate (HFP01SC, Hukseflux), one soil water content, temperature and electrical conductivity sensor (CS655, Campbell Scientific) and one averaging soil thermocouple probe (TCAV, Campbell Scientific). The station is powered by a solar panel and 12V-80Ah battery and data is transmitted to UT-BEG using a cell modem (RV50, Sierra Wireless) and SIM card (McKinney, 2024).

Local rainfall and ET data was used to develop a monthly water budget for the observation period and to estimate total water infiltration. Rainfall and SWC represent hydrological input variables, while ET serves as a key output variable, reflecting the loss of water from the system through evapotranspiration. The rainfall data was used to calculate correlation coefficient between cave drip and antecedent rainfall for 7 - 45 days. Discharge lag times and variations in soil moisture saturation were also evaluated by identifying the maximum correlation coefficient and corresponding time lag, providing a quantitative estimate of the system's hydrologic response time to infiltration events. The daily drip data from each site were plotted against rainfall and soil water content for the hydrological year.

https://doi.org/10.5194/egusphere-2025-2623
Preprint. Discussion started: 2 October 2025

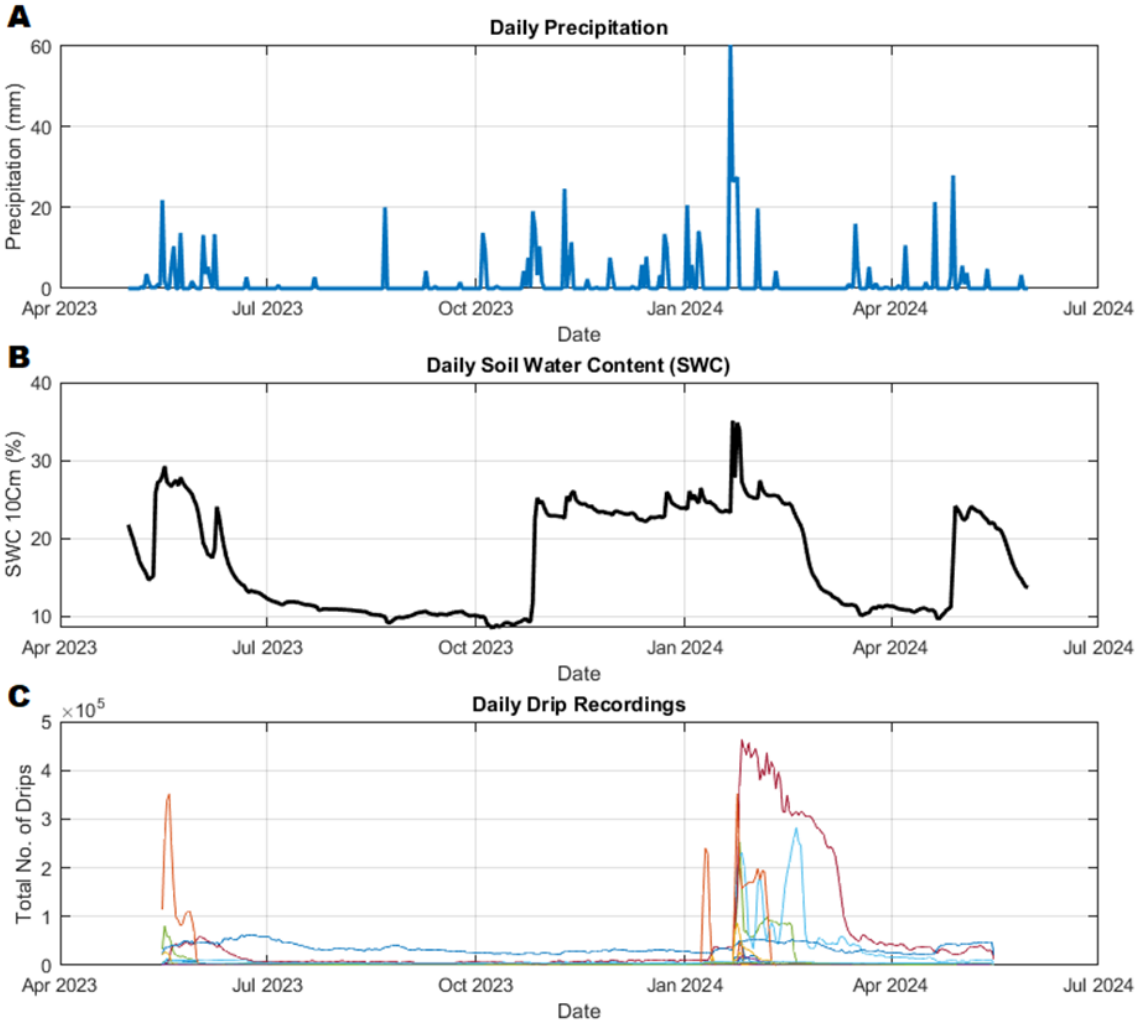

Figure 2: (A) Daily precipitation, (B) SWC, (C) drip time series of all twenty loggers for the entire hydrological year (May 2023 to May 2024).

3.3 Multidimensional scaling (MDS)

Traditional automatic drip discharge analysis has utilized multidimensional scaling (MDS) to investigate the relationship between drip behavior and surface infiltration based on time series analysis (Jex et al., 2012; Mahmud et al., 2018). These methods have been used in conjunction with k-means clustering to examine drip variability and to identify similarities between drip sites (Jex et al., 2012). Similarly, the application of statistical methods to drip water hydrology time series datasets has been used to characterize drip percolation types and classify flow based on drip variability (Mahmud et al., 2018). MDS is a dimensionality reduction technique that embeds high-dimensional data into a lower-dimensional space while preserving the pairwise dissimilarities between items. It starts with a distance matrix, where each value represents the dissimilarity between

https://doi.org/10.5194/egusphere-2025-2623
Preprint. Discussion started: 2 October 2025

two time series, in this case, between two drip loggers. MDS then computes coordinates in a low-dimensional space such that the Euclidean distances between points approximate the original dissimilarities. The result is a spatial layout of the loggers, where proximity reflects similarity in their time series data.

The drip datasets were downloaded as CSV files. A series of analyses were conducted on the drip dataset in RStudio (version 2024.04.2) employing the relevant statistical packages, (e.g., tidyverse for data manipulation, lubridate for date-time processing, stats for ACF and CCF functions and ggplot2 for visualization). MDS was performed considering the average drip rate for each site followed by k-means and hierarchical clustering to identify groupings.

3.4 Cross-correlation

Linear cross-correlation analysis of the daily drip discharge, daily rainfall and daily SWC was conducted to investigate drip water relationships with the climatic variables. This approach allows for the identification of time lags between rainfall, SWC and the corresponding response in drip discharge, helping to reveal the temporal dynamics of water movement through limestone karst. Examining the cross-correlation at various lag intervals (7, 14, 21, 30, and 45-day antecedent period) determines how quickly and to what extent rainfall infiltrates through the karst and influences drip rates, as well as how soil moisture mediates this process. Peak in the cross-correlation indicates the most likely lag time between rainfall (or SWC) and increased drip discharge, revealing insights on subsurface flow pathways and storage behavior within the vadose zone.

3.5 Drip rate vs. overburden thickness

The twenty automatic drip loggers were deployed in rough transects, considering accessibility from the walking trail, the change in ceiling elevation and the locations of actively dripping sites. The estimate of overburden thickness above the cave was obtained from a profile plan of the cave system based on a detailed cave survey and allows us to investigate the impact of the limestone thickness on water infiltration. Loggers 1 to 13 were strategically dispersed within the chamber called the Hall of the Mountain King, the largest room in the cavern, and measures 41 m (135 ft) in depth. We divide this chamber in two sections “Upper Level” and “Lower Level”, in consideration of logger elevation change. Loggers 1 to 10 were positioned in the Upper Level, whereas loggers 11 to 13 were in the Lower Level. On the Upper Level, the ceiling above loggers 1 to 6 has a limestone thickness of 16 m. Accounting for the gradient change, loggers 7 to 10 have an overlying ceiling thickness of 20 m. Loggers 11 to 13 are in the Lower Level and have a thickness of 30 m (logger 11) to 37 m (loggers 12 and 13).

The two loggers positioned at the Emerald Lake section, specifically loggers 13 and 14, have an overburden thickness of 37 m. Loggers l6 to 20 are located in the Castle of the White Giants and have an overburden thickness of 34 m. The influence of elevation variation within the site is observed in the Castle of the White Giants, where higher hydraulic gradient resulted in the largest speleothem features within the cavern. This room is densely packed with huge columns, large chandeliers and a myriad of various stalactite types decorate the ceiling. Stratigraphically, loggers 1 to 10 are situated within the Kainer Formation basal nodular member, and loggers 11 to 20 are within the Glen Rose Formation cavernous member.

https://doi.org/10.5194/egusphere-2025-2623
Preprint. Discussion started: 2 October 2025

4 Results

The actual 15-minute drip logger time series are presented in Fig. S1, with derived statistics in Table 1. Drip volume was calculated considering Genty and Deflandre, (1998), with one drip equal to 0.14 mL. There is significant variability in discharge between the logger locations and within the individual time series evidenced by vast differences in mean discharge rates, skewness, and coefficient of variation (e.g., the mean discharge per 15-min ranges from 0 to 87 mL) (Table 1). We observed mean daily drip rates ranging from 1.84 mL to 8400 mL per day. In terms of standard deviation, logger 14 which also has the highest mean drip rate shows the most variation (standard deviation of 164), while logger 9 presents the lowest drip rate and has the lowest standard deviation of 0.08 (Table 1). The highest COV is 545 at logger 2, indicating that the drip rate is inconsistent or fluctuating abruptly. Logger 20 has the lowest COV value of 20.1, meaning it has the least variability in its drip rate.

https://doi.org/10.5194/egusphere-2025-2623
Preprint. Discussion started: 2 October 2025

Table 1. Calculated statistics for drip sites data logger results

Logger #	Mean drip (ml/per 15 min)	Max drip (ml/per 15 min)	Mean daily drip (ml)	Median daily drip (ml)	Max daily drip (ml)	Standard Deviation (SD)	Co - efficient of Variation (COV)	Skewness	MDS flow classification
Logger 1	2	297	155	11	6795	7	427	18	storage overflow
Logger 2	1	185	108	57	7058	6	545	21	storage overflow
Logger 3	3	47	255	221	3987	3	107	12	storage overflow
Logger 4	0	4	31	31	180	0	82	2	storage overflow
Logger 5	12	535	1197	15	36325	40	323	5	storage overflow
Logger 6	2	7	212	234	406	1	39	0	matrix flow
Logger 7	1	6	106	94	325	0	44	1	storage overflow
Logger 8	2	35	194	17	2807	5	225	4	fracture flow
Logger 9	0	4	2	0	41	0	426	10	storage overflow
Logger 10	2	5	146	139	366	1	40	1	combined flow
Logger 11	3	28	244	113	2600	4	150	4	storage overflow
Logger 12	1	7	133	104	523	1	75	2	combined flow
Logger 13	32	439	3091	930	40477	68	211	4	combined flow
Logger 10	2	5	146	139	366	1	40	1	combined flow
Logger 11	3	28	244	113	2600	4	150	4	storage overflow
Logger 12	1	7	133	104	523	1	75	2	combined flow
Logger 13	32	439	3091	930	40477	68	211	4	combined flow
Logger 14	87	761	8370	1494	66130	164	188	2	combined flow
Logger 15	53	130	5115	4617	9005	16	29	1	combined flow
Logger 16	24	679	2311	5	50494	83	344	4	fracture flow
Logger 17	3	137	264	3	12345	13	479	7	storage overflow
Logger 18	0	37	45	20	492	1	176	6	fracture flow
Logger 19	3	81	318	230	869	3	100	1	combined flow
Logger 20	7	19	685	643	1090	1	20	1	combined flow

https://doi.org/10.5194/egusphere-2025-2623
Preprint. Discussion started: 2 October 2025

4.1 Drip logger and weather data

The analysis of the drip time series in relation to rainfall and SWC reveal useful information into the dynamics of these interactions. We used the optimum frequency of a day according to Mahmud et al, (2016) and plotted the daily time series of drip count with daily precipitation and SWC (Figs. S2 and S3). Most of the loggers responded to extreme rainfall events, such as May 2023 and Jan 2024. However, several loggers show no or little response to rainfall (Fig. S2). Most of the loggers responded to SWC as well but the response was delayed (Fig. S3). To illustrate the observed behavioral patterns, we further change the data frequency to monthly scale and four representative sites have been selected for presentation (Fig. 3). Many loggers exhibit relatively instantaneous (e.g., logger 4) or delayed (e.g., logger 14) responses to rainfall on a monthly scale, with the January 2024 peak being a notable example (Fig. 3A). Few loggers (such as loggers 6 and 20), show more variable responses, suggesting that certain drips may not be directly linked to rainfall. The relationship between SWC and infiltration is somewhat evident, with drip counts for loggers 8 and 19 displaying observed trending (Fig. 3B). In contrast, loggers 6 and 20 demonstrate a weaker correlation with SWC, similar to rainfall, which may imply that the water supply is originating from alternative sources, such as seepage from overlying limestone, overflow of stored water, or lateral groundwater flow.

https://doi.org/10.5194/egusphere-2025-2623
Preprint. Discussion started: 2 October 2025

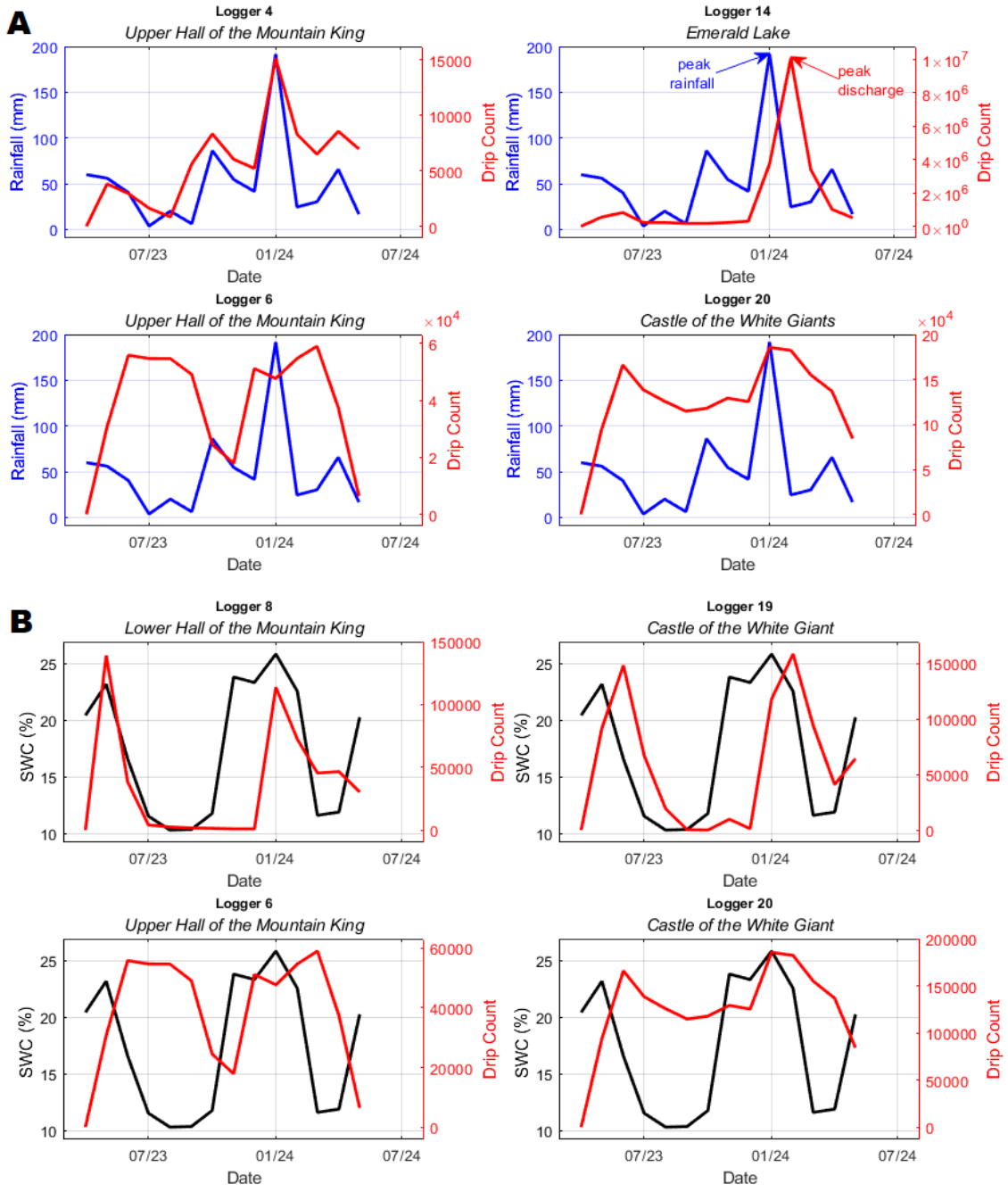

Figure 3: Monthly drip responses across different loggers, highlighting the relationship between drip count and (A) Rainfall and (B) SWC within 10 cm of topsoil.

https://doi.org/10.5194/egusphere-2025-2623
Preprint. Discussion started: 2 October 2025

4.2 MDS clustering

MDS clustering identified four distinct clusters, a finding which agrees with that of Mahmud et al. (2018). These clusters were determined based on the constructed hierarchical dendrogram (Fig. S4A). The choice of four clusters was supported by examining the significant splits. The scatter plot (Fig. S4B), indicates that a four-cluster solution best captures the underlying structure in the data. These clusters can be attributed to different flow dynamics and were used to classify flow types. In order to visualize the drip time series, the flow-rate log plot highlights individual loggers within the obtained cluster groupings (Fig. 4). The plots reveal distinguishable patterns across the different drip time series.

Matrix flow (Cluster 1 in Fig. 4A) is characterized by sustained drip rates punctuated by slight decreases and subdued responses that do not reflect the contributions of rainfall events. This indicates percolation with limited influence from preferential pathways or precipitation indicating strong storage capacity and attenuation of input signals. The relationship between variables follows a similar trend for the various clusters, characterized by corresponding patterns. This suggests a shared underlying process or behavior across the drip loggers. Despite variations in magnitude, the alignment of time series along comparable trajectories indicates a strong similarity in the dynamics being observed. Fracture flow (Cluster 2 in Fig. 4B) exhibits a drip pattern overlaid with rapid, high-intensity responses punctuated by peaks that correspond to rainfall events. Combined flow (Cluster 3 in Fig. 4C) typically represents an interaction between diffuse and preferential flow pathways. The time series displays a consistently higher drip rate along with a steady base flow signal and sharp spikes in drip rate that correspond to increases in percolation. The presence of both slow and fast components in the drip time series suggests that this flow type is influenced by both storage-driven and direct recharge mechanisms. The storage overflow (Cluster 4 in Fig.4D) displays sudden and pronounced increases in drip rate in response to periods of heavy rainfall. This typically reflects the point at which the epikarst or overlying rock reaches saturation, leading to rapid discharge through preferential flow paths. A lag between peak rainfall and the onset of overflow is also seen, followed by a gradual return to baseline levels.

https://doi.org/10.5194/egusphere-2025-2623
Preprint. Discussion started: 2 October 2025

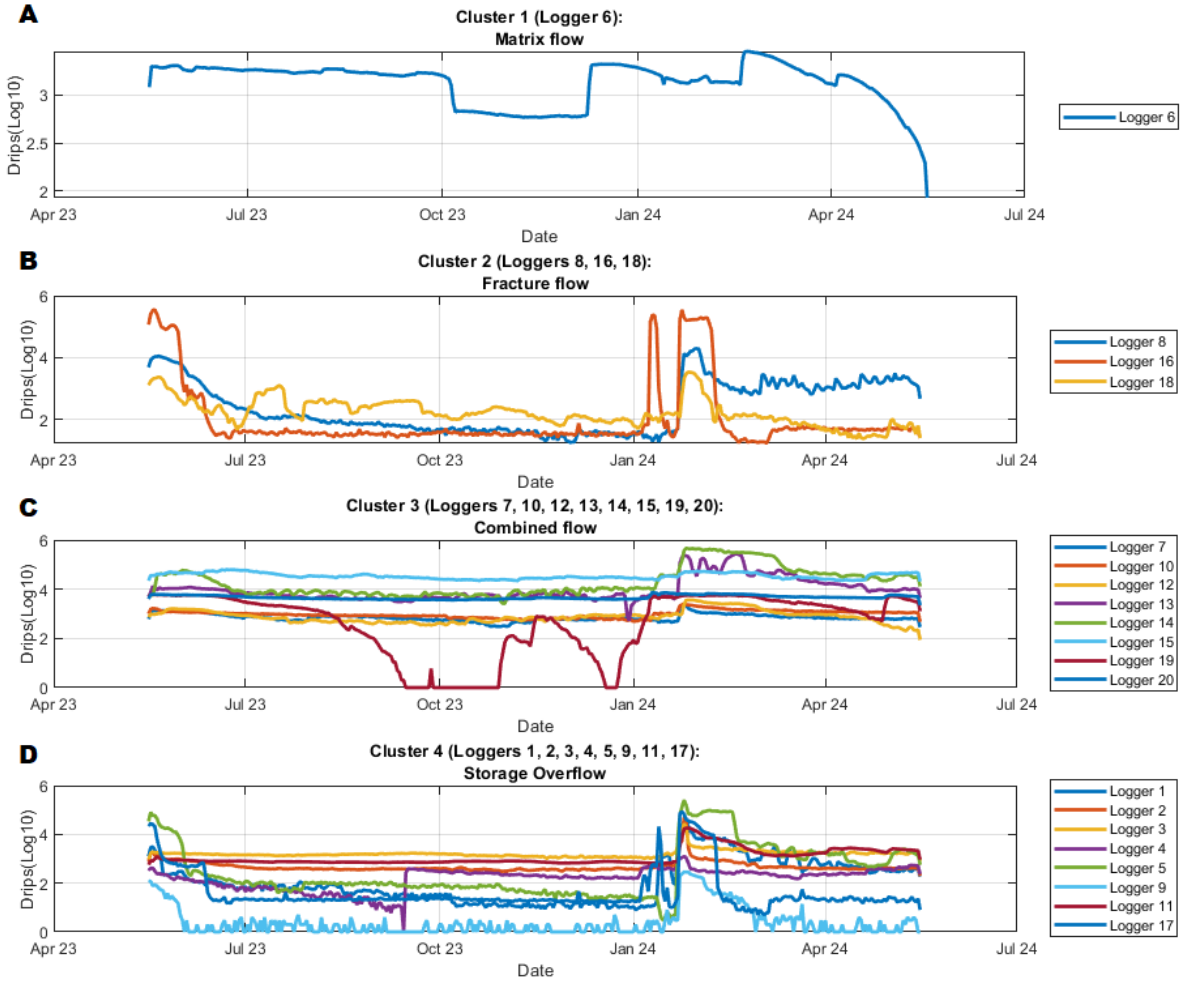

Figure 4: Daily drip count time series separated by different cluster groups or flow classification. (A) Matrix flow. (B) Fracture flow. (C) Combined flow. (D) Storage overflow

4.3 Cross-correlation analysis

Cross-correlation was plotted for each drip logger compared against rainfall (Fig. S5) and SWC (Fig. S6) to examine the correlation at shifting daily lags up to 45 days. The analysis showed that the drip time series and antecedent rainfall maintained a highly correlated relationship up to 14 days. The strongest associations were for the 7-day antecedent period. Matrix flow displays the lowest correlation, 0.02 (Fig. S5). This low value indicates no meaningful correlation between antecedent rainfall and drip rates at this site. This suggests that drip water at this location does not respond to rainfall and may be influenced by other variables, such as being fed by steady percolation through permeable rock or drip discharge governed by slow matrix drainage. Correlation for the fracture flow grouping had a range of 0.36 to 0.38 (Fig. S5). Observed lag between peak rainfall and drips has a median value of 13 days (Fig. S5). This moderate positive correlation indicates that rainfall does influence drip,

https://doi.org/10.5194/egusphere-2025-2623
Preprint. Discussion started: 2 October 2025

but the relationship is somewhat variable and there is most likely a subsurface-driven hydrological response, with drips fed by preferential flow paths via conduits. The combined flow displayed correlation values ranging from 0.10 to 0.29 and had a 12-day lag (Fig. S5). This represents a weak positive relationship, indicating that there is only a slight tendency for rainfall to affect drip rates. Drip discharge at these locations is not closely associated with rainfall, such that drip water is either sourced from multiple infiltration points or by mixing with recharge, reflecting a composite signal. Alternatively, the sites may require multiple rainfall events to saturate before flow initiates alongside storage-dominated behavior in the epikarst, with threshold-controlled release. The highest correlation observed were for the storage overflow cluster which ranged from 0.41 to 0.59, a moderate positive correlation with a median observed lag of 11 days (Fig. S5). This suggests that antecedent precipitation has a noticeable impact on drip rates for these locations and significantly influences the hydrological response. Discharge is likely governed by infiltration, moisture levels and the subsurface dynamics required for rainfall alongside stored water within the epikarst to percolate and contribute to dripping.

The drip timeseries and antecedent SWC cross-correlation analysis showed that they were highly correlated up to 7 days (Fig. S6). The drip loggers with the lowest r values were loggers 2, 3, 6, 10, and 18 which ranged from 0.21 to 0.27. This represents a weak positive correlation, indicating that there is only a slight tendency for SWC to affect drip rates at these locations. The strongest values observed were for drip loggers 4, 5, 12, 14, 19, and 20 ranging from 0.42 to 0.61, a moderate positive correlation (Fig. S6). This suggests that SWC had a noticeable impact at these sites. The second strongest r values were for loggers 1, 7, 8, 9, 11, 13, 16, and 17 with a range of 0.32 to 0.38 (Fig. S6). The correlation groupings for antecedent SWC did not align with the observed pattern based on flow classification as seen with antecedent rainfall. Instead, it displays a more erratic distribution, therefore the SWC variability does not reflect the distinctions needed to support classification grouping and could not be used as a supporting parameter.

4.4 Drip behavior vs overburden thickness

Figure 6 displays the relationship between mean drip per 15 min, skewness, and COV against the overburden thickness. Typically, shallower sites are associated with a higher maximum drip rate, mean and standard deviation versus deeper sites (Markowska et al., 2015). This depth relationship and the influence of bedrock is not observed at NBC. For example, logger 17, which is located in the deeper Castle of the White Giants was clustered with the shallower sites (Fig. 5B) despite its estimated overburden thickness of 35 m. However, logger 6 is excluded from that cluster group, notwithstanding its location in the shallow Hall of the Mountain King proximal to those loggers (Fig. 5A). The designation of matrix flow is assigned to shallow drip sites and fracture flow to the deeper sites. Where the overburden thickness is thinner drips are slower and where the overburden is thicker, flow is faster (Fig. 5B). This further supports the assumption that overburden over the Castle of the White Giants is more fractured, has more infiltration flow paths and increased potential vadose-zone storage volume.

Skewness and COV for the matrix flow are low, which has an overburden thickness of 16 m. A near zero skewness means the drip rate distribution is symmetric and there are no strong spikes or extremes. This indicates no strong or sudden response to individual rainfall events, instead the drip flow is steady and gradually changes over time. The COV points to very low

https://doi.org/10.5194/egusphere-2025-2623
Preprint. Discussion started: 2 October 2025

variability at this site with drips at a nearly constant rate. This is typically for matrix-dominated flow and associated with longer water residence times. The fracture flow group has a skewness and COV within a range of 4 to 6 and 176 to 344 respectively and overburden across these sites ranges from 20-34 m. Here we observe all positively skewed values indicating episodic dripping with some sharp responses to rainfall, including short bursts of elevated drip activity and high variability, exhibiting more event driven behavior. Discharge at drip points occurs when the epikarst becomes saturated enough to initiate percolation or storage thresholds are surpassed. The overburden thickness is 20 to 37 m for the combined flow with a skewness ranging between 1 to 10 and COV changes within 29 to 426, representing a diverse mix of flow behaviors across the drip sites. Again, all values are positively skewed. The wide skewness suggests that some sites are controlled by matrix and epikarst storage and others are influenced by discrete threshold-controlled fracture flow, where recharge begins only after reaching a saturation point. This reflects a dual-flow regime: structural heterogeneity governs the balance between storage-dominated and event-responsive drip behaviors. The storage overflow group has a 16 to 34 m overburden, skewness ranges from 2 to 21 and COV changes from 39 to 545. All values are positively skewed, indicating episodic, irregular flow dominated by occasional high-drip events, with fluctuating drip responses dependent on the connectivity of recharge pathways. Drip patterns align with rainfall, while response variability reflects storage-controlled flow to rapid event-driven dripping, supporting threshold-driven flow.

https://doi.org/10.5194/egusphere-2025-2623
Preprint. Discussion started: 2 October 2025

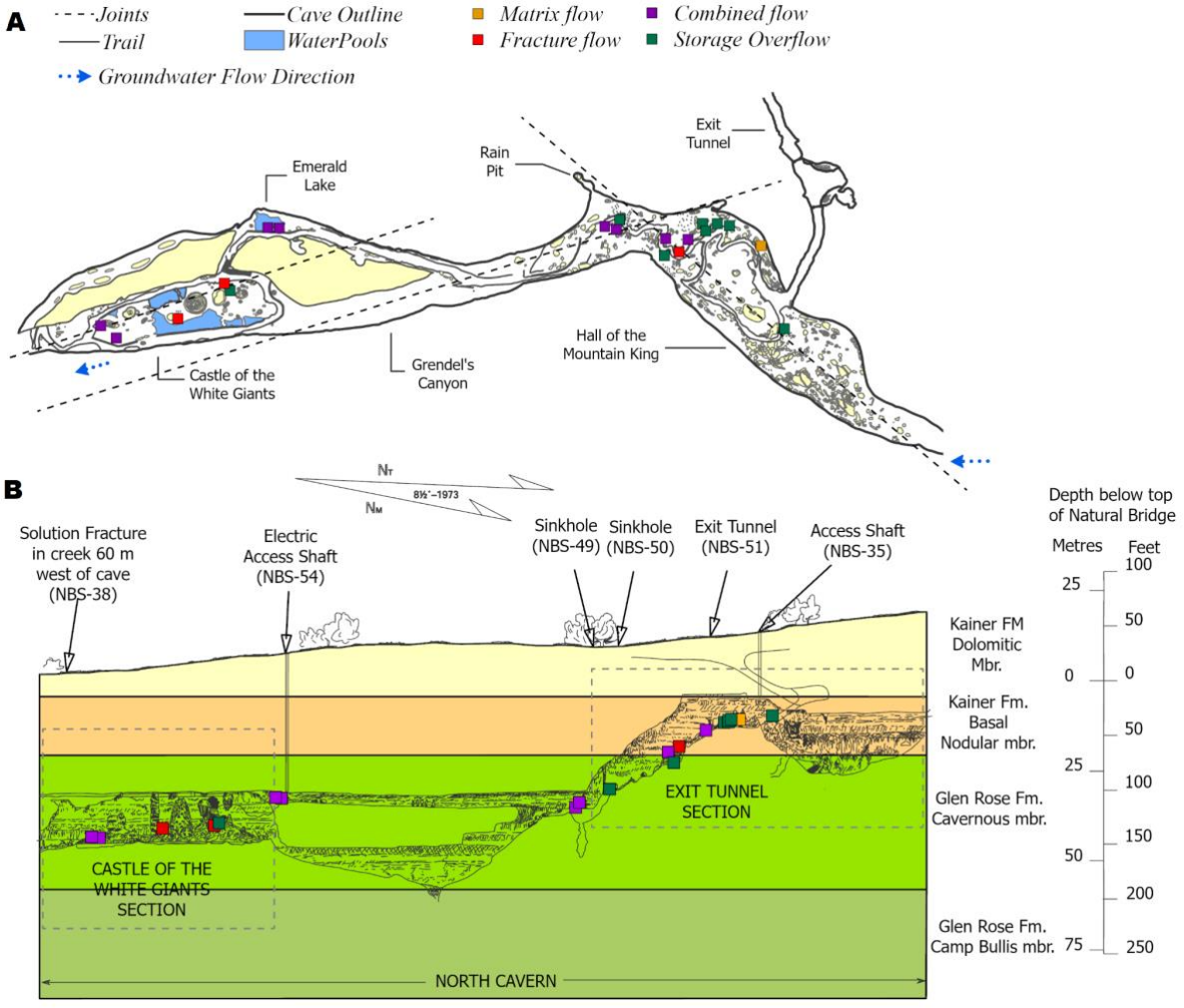

Figure 5: (A) Plan and (B) Depth Profile of NBC showing cluster groups or flow classification for drip loggers. Loggers are indicated by colored squares, with orange corresponding to matrix flow, red - fracture flow, purple - combined flow and green - storage overflow.

https://doi.org/10.5194/egusphere-2025-2623
Preprint. Discussion started: 2 October 2025

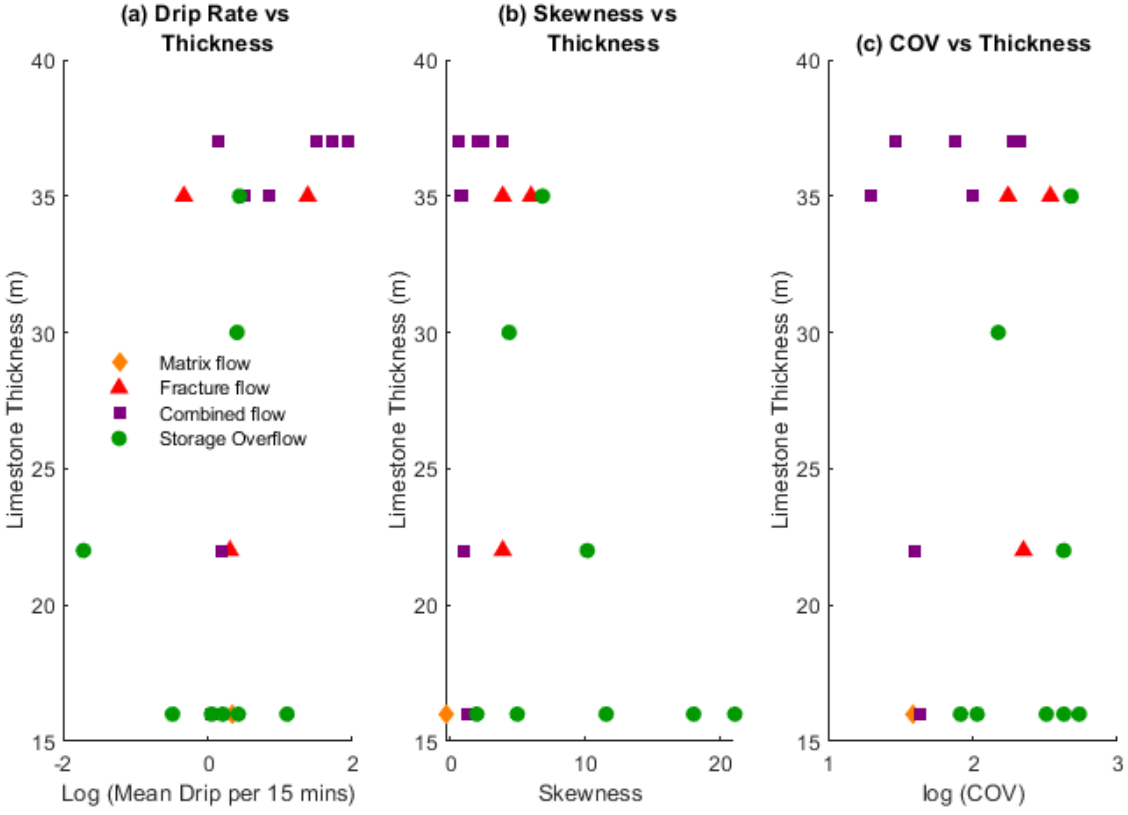

Figure 6: (A) Limestone thickness versus mean discharge. (B) Skewness versus depth showed no relationship; however, it did indicate that all sites exhibited a positive skew, suggesting that lower discharge rates prevailed, occasionally interrupted by brief periods of high discharge. (C) Coefficient of Variation (COV) versus thickness also displayed no association, implying that variance does not change with depth.

5 Discussions

The cave drip time series presented here demonstrate the heterogeneities that exist in drip behavior across different loggers within the same cave during a one-year period. Drip discharge generally decreased during the dry season (summer months) at most sites, with the exception of a few loggers (Fig. S1). The functional mean plot (Fig. 7A) represents the average drip rate trajectory across all logger sites over the observation period. The mean curve remains consistently above zero, reinforcing the observation of continuous dripping at all monitored sites, regardless of short-term environmental variability. The long-term discharge time-series shows a relationship with the water budget (Fig. 7B), exhibiting a decline during moisture-deficit period, and high flow through phases of positive water balance. All twenty loggers remained active throughout the study, reflecting a significant storage component similar to the observations of Smart and Freiderich (1987), Baker et al., (1999), Baker and Brunsdon, (2003), Tooth and Fairchild,(2003), and have been visualized against daily rainfall (Fig. S2). Similar to previous research findings (McDonald and Drysdale, 2007; Jex et al., 2012; Mahmud et al., 2018), the drips studied at NBC's Discovery

https://doi.org/10.5194/egusphere-2025-2623
Preprint. Discussion started: 2 October 2025

Passages show substantial spatial and temporal differences in the drip discharge (Fig. S1), highlighting the complexity of hydrological linkages between the two large chambers.

Logger 6 in particular, registered a continuous response and exceptionally low correlation with rainfall (Fig. S2) and SWC (Fig. S3), suggesting that the water source is relatively stable and unaffected by short-term precipitation events. The logger exhibits continuous drips signifying that this area might be drawing water from multiple sources, potentially influenced by variations in hydraulic piston flow (Smart and Friederich, 1987). The discharge behavior is characterized by low variability and is distinct from other drips (Fig. S1). This type of response is likely influenced by the flow paths, typical of matrix flow, which displays minimal sensitivity to short term rainfall events, remaining consistent over time. The recharge-discharge pattern is disconnected from rainfall, supporting a likely source from epikarst groundwater.

For the four groupings derived from MDS, Cluster 1 or matrix flow (Fig. 5A) exhibits a persistent base flow component with steady discharge and no discernible relationship with hydrologically effective precipitation. Water enters the system consistently at this location, most likely driven by matrix flow from the surrounding rock. Matrix flow tends to be slower (212 mL/day) and can maintain consistent water release as drips (COV = 4 - 6) even in periods without significant rain, as groundwater stored in the rock matrix slowly moves from the surface. The persistent base flow observed in the drip data reflects slow and continuous water movement, possibly sustained groundwater contribution from the vadose, even when there are no immediate precipitation events. Cluster 2 or fracture flow (Fig. 5B) has static drips with some discernible variation through time (COV = 176 - 344) and moderate flow rates (850 mL/day) but high response to rainfall events, particularly those of May 2023 and Jan 2024 and a few smaller ones between these dates. It represents the loggers with a fast response to surface infiltration, presumably via a fracture network, or disconnected fractures that behave similarly (Jex et al., 2012). Drip loggers classified as fracture flow have fast drip rates in response to rainfall, however low drip discharge during dry periods. Cluster 3 or combined flow (Fig. 5C) represents high-variability drips (COV = 29 - 426) with high discharges (2496 mL/day), and constant flow rates, except for logger 19. This group displays a lower rainfall response. Frequent decreases along with high variability may be indicative of flow switching between different reservoirs and indicates significant complexity in the drip behavior at these sites (McDonald and Drysdale, 2007). Cluster 4 or storage overflow (Fig. 5D) shows medium-variability drips (COV = 39 - 545) with low discharges (282 mL/day). For sites within this group, high response levels coincide with two periods of heavy rainfall, in May 2023 and Jan 2024, this could indicate that either a threshold is required to trigger an increase in discharge through overflow, or that the hydraulic head is influencing a change in the source (Smart and Friederich, 1987; Tooth and Fairchild, 2003). With regard to the general clustering the influence of storage overflow and matrix flow (Fig. 5B) is more prevalent in the Hall of the Mountain King. The Castle of the White Giants and the Emerald Lake host combined flow and fracture flow (Fig. 5B). These drip time series show significant variations in their base flow and response intensity (Fig. 4). The observed variability is typical to that of previous studies using drip loggers (Jex et al., 2012; Markowska et al., 2015; Mahmud et al., 2016; Chapman et al., 2024).

Cross correlation results for rainfall (Fig. 8) could possibly act as a proxy to illustrate the expected ranges for the different flow classification types. The near zero correlation obtained for matrix flow (0.02) indicates minimal hydraulic connection to

https://doi.org/10.5194/egusphere-2025-2623
Preprint. Discussion started: 2 October 2025

surface rainfall events. The fracture flow group's moderate correlations (0.36 - 0.38) imply a more rapid but not instantaneous response to rainfall. This aligns with water moving through fractures that typically transmit flow faster than the matrix but with some observed delay or attenuation. Combined flow values (0.10 - 0.29) suggest a mixture of matrix and fracture contributions. The wide range reflects variability in the degree of connectivity and the proportion of fast versus slow flow components. Storage Overflow has the highest correlation values (0.41 - 0.59) indicating a relatively strong response to rainfall, likely due to stored water being mobilized during recharge events. This suggests the presence of epikarst reservoirs that release water rapidly once thresholds are reached.

The slower matrix and storage overflows are lithologically associated with the Kainer Formation, Basal Nodular member. However, faster fracture and combined flow sites occur within the Glen Rose Formation Cavernous member (Fig. 5B). The cave drips reaching at the Hall of the Mountain King ceiling infiltrate through the Dolomitic member of Kainer Formation, consisting of thicker limestone beds with restricted porosity (Fig. 5B). In contrast, the cave drips reaching at the castle of the White Giants ceiling pass through a thin layer of Dolomitic member and thicker layers of Basal nodular member of Kainer Formation and Cavernous member of Glen Rose Formation (Fig. 5B). Both the Basal nodular member and Cavernous member have developed extensive secondary porosity. This secondary porosity primarily drives the water flow, not the overburden thickness. More water is driven through the secondary porosity of the Castle of the White Giants, despite having a thicker overburden. There is no observable relationship between drip rate and overburden thickness. Based on flow classification, combined flow has the highest flow while matrix and storage are significantly lower. This supports a highly heterogeneous, fractured karst system at NBC's Discovery Passages. Moreover, infiltration rates have been calculated as 2.9 m/day for the Castle of the White Giants (mainly driven by fracture and combined flows) and 1.3 m/day for the Hall of the Mountain King (characterized by storage overflow). These values represent the heterogeneous nature of infiltration in karst systems, highlighting the dominance of preferential flow paths such as fractures and conduits at the deeper cave section in the Castle of the White Giants. The lower infiltration rate observed at the Hall of the Mountain King suggests slower water movement due to low porous water retention within the vadose zone. Overall, the infiltration rates support the interpretation of dynamic recharge processes and emphasize the importance of distinguishing between flow regimes when evaluating karst hydrology.

Interpreting drip behavior alongside overburden thickness can reveal insights about the hydrological response capacity of the rock material above the studied cave sections. With a thinner overburden for the shallow cave section, there is less rock and soil to buffer or store infiltrating water. It is expected that rainfall reaches these locations quicker, possibly via direct fracture/conduit pathways. Drip time series is usually flashier with rapid spikes following rainfall. The Hall of the Mountain King has a moderately shallow overburden of 16 m and a relatively low skewness range of 2 to 21. Values are positively skewed, indicating irregular flow dominated by occasional high-drip events. This location is controlled by matrix/porous flow representing water flowing down and seeping through rock matrix. A thicker overburden for the deeper cave section, the Castle of the White Giants, means there is more rock material for water storage and delay, especially within the epikarst. Infiltrating water takes longer to reach the cave, and the drip time series displays higher variability. Skewness values suggest the site is

https://doi.org/10.5194/egusphere-2025-2623
Preprint. Discussion started: 2 October 2025

more responsive to individual rain events with drip rates that vary significantly over time. This section, therefore, is dominated by fracture flow.

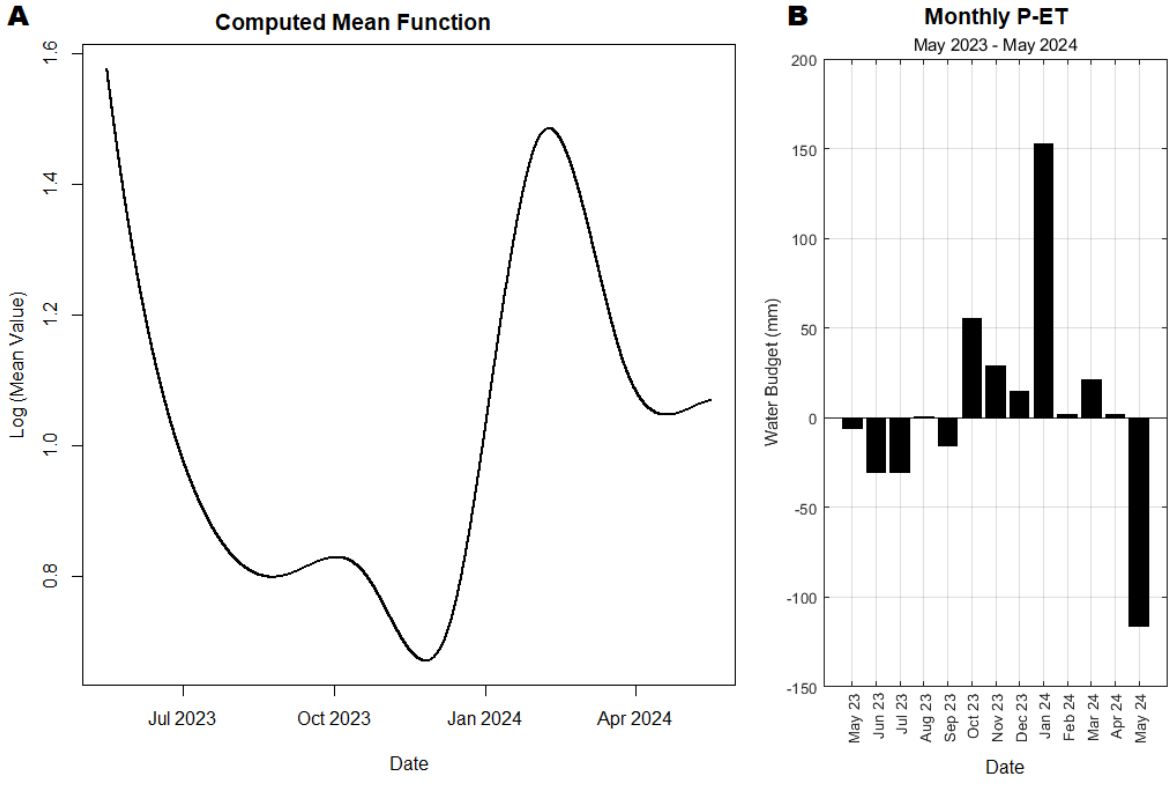

Figure 7: (A) Functional mean of all NBC drip sites across time. (B) Calculated water budget

https://doi.org/10.5194/egusphere-2025-2623
Preprint. Discussion started: 2 October 2025

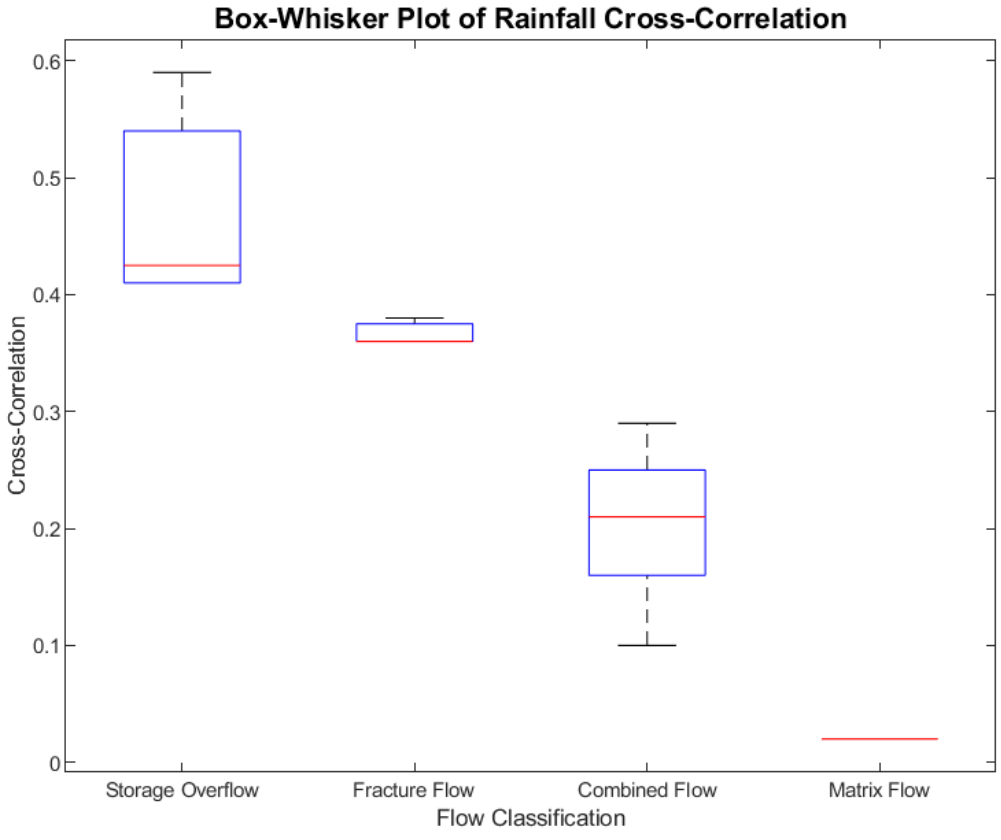

Figure 8: Box plots showing the results of the rainfall cross-correlation analysis

6 Conclusions

The drip time series obtained from monitoring twenty loggers at NBC's Discovery Passages displays a diverse range of characteristics as it relates to discharge. This is analogous to other similar studies (Tooth and Fairchild, 2003; Baker and Brunsdon, 2003; McDonald and Drysdale, 2007; Jex et al., 2012; Markowska et al., 2015; Mahmud et al., 2018). The differences in discharge patterns among drip sites alludes to the local complexity of hydrological pathways within this karst system. There is a strong likelihood of storage reservoirs feeding some locations and a general upsurge in observed discharge with increasing overburden thickness of the karst formation. McDonald and Drysdale (2007) determined that the delivery mechanism to each drip logger is additionally influenced by increasing bedrock depth and the capacity for mixing of water sources.

The observed behavior supports the complex nature of the karst hydrology, as proximal loggers may differ significantly (McDonald and Drysdale (2007). Drip loggers in the near-surface Hall of the Mountain King respond and are classed similarly,

https://doi.org/10.5194/egusphere-2025-2623
Preprint. Discussion started: 2 October 2025

as being matrix and storage overflow dominated. Accordingly, this implies a higher degree of flow path interconnectivity and simpler bedrock structure (Tooth and Fairchild, 2003). This supports the idea that flow paths are influenced by the fracture pathways for the different formations. Therefore, the different limestone formations within NBC might affect infiltration. The Upper Glen Rose Formation is inherently easier to permeate with enhanced fractures – it has a laminar structure, exhibits less grain-size variation relative to the Kainer Formation. It is underlain by evaporite-rich deposits that promote downward collapse. Although Genty and Deflandre, (1998) have indicated that one hydrological year is sufficient to understand the water flow dynamics at any particular cave, there are notable limitations. This study captures a short window of the climatic variability of the region, covering a relatively dry period, during which time there was extreme drought conditions as indicated by the EAA J-17 index well. As such, it cannot be definitely concluded whether the observations for this site from May 2023 to May 2024 sufficiently reflect the general response for this limestone formation. However, it can be noted that the analysis of the time series produced by cave drip loggers has generated some useful hydrogeological information. This technique can be applied for a longer time period at NBC's Discovery Passages once more data is available due to continuous measurement of the drip loggers. Moreover, this methodology can be applied globally for drip logger data collected in any cave site.

This study highlights the need for the continued long-term, high-resolution monitoring of cave drip water to 1.) accurately characterize the temporal variability, 2.) assess the influence of climatic factors and karst, and 3.) to understand the governing hydrological processes of recharge mechanisms, water residence times, and flow rate variations. Such continuous monitoring would facilitate a deeper understanding of the key factors driving drip discharge variability, including seasonal shifts in precipitation and temperature as a result of wet (La Niña) or dry (El Niño) years, subsurface flow dynamics within the karst system, and the influence of SWC and ET. Additionally, the interactions between these factors can provide insights into the hydrological connectivity between surface and subsurface environments, helping to clarify the impacts of episodic events and long-term trends on cave drip behavior. With ongoing data collection from automated drip loggers, coupled with statistical data analysis techniques, we can gain a more comprehensive understanding of the intricate interactions between cave environments and groundwater systems. This will enable more accurate assessments of hydrological processes, such as drip rate fluctuations, recharge patterns, and subsurface flow dynamics, ultimately leading to improved predictions and more effective management strategies for these critical natural resources. In conclusion, MDS demonstrates significant potential for classifying and visualizing the complex relationships between water infiltration processes and the underlying fractured limestone matrix. By representing these spatial and temporal variations in a reduced dimensionality, MDS facilitates the identification of patterns in the data. Additionally, hierarchical clustering techniques provide optimal groupings within the cave drip time series, enabling the identification of distinct trends in drip behavior that are influenced by variations in water flow pathways, fracture networks, and other subsurface properties.

https://doi.org/10.5194/egusphere-2025-2623
Preprint. Discussion started: 2 October 2025

References

Baker, A., and Brunsdon, C., 2003, Non-linearities in drip water hydrology: an example from Stump Cross Caverns, Yorkshire: Journal of Hydrology, v. 277, p. 151–163, doi:10.1016/S0022-1694(03)00063-5.

Baker, A., Barnes, W.L., and Smart, P.L., 1997, Variations in the discharge and organic matter content of stalagmite drip waters in Lower Cave, Bristol: Hydrological Processes, v. 11, p. 1541–1555, doi:10.1002/(SICI)1099-1085(199709)11:11<1541::AID-HYP484>3.0.CO;2-Z

Baker, A., Berthelin, R., Cuthbert, M.O., Treble, P.C., Hartmann, A., and the KSS Cave Studies Team, 2020, Rainfall recharge thresholds in a subtropical climate determined using a regional cave drip water monitoring network: Journal of Hydrology, v. 587, p. 125001, doi:10.1016/j.jhydrol.2020.125001.

Baker, A., Scheller, M., Oriani, F., Gregoire, M., Hartmann, A., Wang, Z., and Cuthbert, M.O., 2021, Quantifying temporal variability and spatial heterogeneity in rainfall recharge thresholds in a montane karst environment: Journal of Hydrology, v. 594, p. 125965, doi:10.1016/j.jhydrol.2021.125965.

Baldini, J.U.L., McDermott, F., and Fairchild, I.J., 2006, Spatial variability in cave drip water hydrochemistry: Implications for stalagmite paleoclimate records: Chemical Geology, v. 235, p. 390–404, doi:10.1016/j.chemgeo.2006.08.005.

Barker, R.A., Bush, P.W., and Baker, E.T., 1994, Geologic history and hydrogeologic setting of the Edwards-Trinity aquifer system, west-central Texas: US Geological Survey, doi:10.3133/wri944039.

Bauer, S., Liedl, R., and Sauter, M., 2005, Modeling the influence of epikarst evolution on karst aquifer genesis: A time-variant recharge boundary condition for joint karst-epikarst development: Water Resources Research, v. 41, doi:10.1029/2004WR003321.

Bruun, B., Jackson, K., and Lake, P., 2016, Texas Aquifers Study: Groundwater Quantity, Quality, Flow, and Contributions to Surface Water: KIP Articles. 4891.https://digitalcommons.usf.edu/kip_articles/4891/ (accessed November 2024).

Campbell, M., Callow, J.N., McGrath, G., and McGowan, H., 2017, A multimethod approach to inform epikarst drip discharge modelling: Implications for palaeo-climate reconstruction: Hydrological processes, v. 31, p. 4734–4747, doi:10.1002/hyp.11392.

Chapman, R.G., Laffan, S., McDonough, L.K., Markowska, M., and Baker, A., 2024, Spatiotemporal variation in cave percolation waters: A functional approach: Journal of Hydrology, v. 631, p. 130784, doi:10.1016/j.jhydrol.2024.130784.

Collins, E.W., 1998, Environmental Geology of Urban Growth Areas Within the Edwards Aquifer and Balcones Fault Zone, South-Central Texas: Gulf Coast Association of Geological Societies Transactions, v. 48, https://archives.datapages.com/data/gcags/data/048/048001/0537.htm (accessed May 2024).

Collins, E.W., and Hovorka, S.D., 1997, Structure Map of the San Antonio Segment of the Edwards Aquifer and Balcones Fault Zone, South-Central Texas: Structural Framework of a Major Limestone Aquifer: Kinney, Uvalde, Medina, Bexar, Comal, and Hays Counties:, https://digitalcommons.usf.edu/kip_articles/5312/ (accessed May 2024).

https://doi.org/10.5194/egusphere-2025-2623
Preprint. Discussion started: 2 October 2025

Collister, C., and Mattey, D., 2005, High resolution measurement of water drip rates in caves using an acoustic drip counter: AGU Fall Meeting Abstracts, v. 2005, p. PP31A–1496, https://ui.adsabs.harvard.edu/abs/2005AGUFMPP31A1496C/abstract.

Elliott, W.R. & Veni, G., 1994, The caves and karst of Texas. National Speleological Society Convention Guidebook: Huntsville, Alabama, 342 pp.

Fairchild, I.J., and Baker, A., 2012, Speleothem science: From process to past environments: Chichester, England, Wiley-Blackwell, Blackwell Quaternary Geoscience Series, 450 p., doi:10.1002/9781444361094.

Ferrill, D.A., Sims, D.W., Waiting, D.J., Morris, A.P., Franklin, N.M., and Schultz, A.L., 2004, Structural framework of the Edwards Aquifer recharge zone in south-central Texas: GSA Bulletin, v. 116, p. 407–418, doi:10.1130/B25174.1.

Ford, D., and Williams, P., 2013, Karst Hydrogeology, in Karst Hydrogeology and Geomorphology, John Wiley & Sons, Ltd, p. 103–144, doi:10.1002/9781118684986.ch5.

Gary, M.O., 2011, Geologic Assessment for Natural Bridge Caverns Comal County, Texas: Zara Environmental LLC, 40

Genty, D., and Deflandre, G., 1998, Drip flow variations under a stalactite of the Père Noël cave (Belgium). Evidence of seasonal variations and air pressure constraints: Journal of hydrology, v. 211, p. 208–232, doi:10.1016/s0022-1694(98)00235-2.

Goldscheider, N., Chen, Z., Auler, A. S., Bakalowicz, M., Broda, S., Drew, D., Hartmann, J., Jiang, G., Moosdorf, N., Stevanovic, Z., Veni, G., 2020, Global distribution of carbonate rocks and karst water resources: Hydrogeology Journal, v. 28, p. 1661–1677, doi:10.1007/s10040-020-02139-5.

Heidemann C., 1995, Natural Bridge Caverns, Handbook of Texas Online: Published by Texas State Historical Association: https://www.tshaonline.org/handbook/entries/natural-bridge-caverns (accessed March, 2023).

Jex, C.N., Mariethoz, G., Baker, A., Graham, P., Andersen, M.S., Acworth, I., Edwards, N., and Azcurra, C., 2012, Spatially dense drip hydrological monitoring and infiltration behaviour at the Wellington Caves, South East Australia: International Journal of Speleology, v. 41, p. 14, doi:10.5038/1827-806X.41.2.14.

Kastning, E. H., 1983, Geomorphology and Hydrogeology of the Edwards Plateau Karst, Central Texas [Ph.D. dissertation]: University of Texas at Austin, 280 p., Texas Speleological Survey reissue, 2015., p.149-164 https://www.texasspeleologicalsurvey.org/PDF/Kastning.pdf

Klimchouk, A.B., 2015, The Karst Paradigm: Changes, Trends and Perspectives: Acta Carsologica, v. 44, doi:10.3986/ac.v44i3.2996.

Klimchouk, A.B., 2004, Towards defining, delimiting and classifying epikarst: Its origin, processes and variants of geomorphic evolution: Epikarst. Special Publication, v. 9, p. 23–35, https://www.karstwaters.org/wp-content/uploads/2023/06/SP9-Epikarst.pdf#page=30.

Lindgren, R.J., Dutton, A.R., and Hovorka, S.D., 2004, Conceptualization and simulation of the Edwards aquifer, San Antonio region, Texas:, https://digitalcommons.usf.edu/kip_articles/1146/ (accessed November 2024).

https://doi.org/10.5194/egusphere-2025-2623
Preprint. Discussion started: 2 October 2025

Li, P., Tian, R., Xue, C., and Wu, J., 2017, Progress, opportunities, and key fields for groundwater quality research under the impacts of human activities in China with a special focus on western China: Environmental Science and Pollution Research, v. 24, p. 13224–13234, doi:10.1007/s11356-017-8753-7.

Maclay, R.W. and Small, T.A., 1986, Carbonate Geology and Hydrology of the Edwards Aquifer in the San Antonio Aquifer Area, Texas: Texas Water Development Board Report no. 296, 90 p.

Mahmud, K., Mariethoz, G., Baker, A., and Treble, P.C., 2018, Hydrological characterization of cave drip waters in a porous limestone: Golgotha Cave, Western Australia: Hydrology and Earth System Sciences, v. 22, p. 977–988, doi:10.5194/hess-22-977-2018.

Mahmud, K., Mariethoz, G., Baker, A., Treble, P.C., Markowska, M., and McGuire, E., 2016, Estimation of deep infiltration in unsaturated limestone environments using cave lidar and drip count data: Hydrology and Earth System Sciences, v. 20, p. 359–373, doi:10.5194/hess-20-359-2016.

Mariethoz, G., Baker, A., Sivakumar, B., Hartland, A., and Graham, P., 2012, Chaos and irregularity in karst percolation: Geophysical Research Letters, v. 39, doi:10.1029/2012GL054270.

Markowska, M., Baker, A., Treble, P.C., Andersen, M.S., Hankin, S., Jex, C.N., Tadros, C.V., and Roach, R., 2015, Unsaturated zone hydrology and cave drip discharge water response: Implications for speleothem paleoclimate record variability: Journal of Hydrology, v. 529, p. 662–675, doi:10.1016/j.jhydrol.2014.12.044.

McDonald, J., and Drysdale, R., 2007, Hydrology of cave drip waters at varying bedrock depths from a karst system in southeastern Australia: Hydrological Processes, v. 21, p. 1737–1748, doi:10.1002/hyp.6356.

McKinney, S., 2024, Edwards Aquifer Authority Cibolo (US-EA4), Uvalde (US-EA5), and Nueces (US-EA6) Data (2021-2023), doi:10.18738/T8/1NSBMG.

McMahon, P.B., Plummer, L.N., Böhlke, J.K., Shapiro, S.D., and Hinkle, S.R., 2011, A comparison of recharge rates in aquifers of the United States based on groundwater-age data: Hydrogeology Journal, v. 19, p. 779–800, doi:10.1007/s10040-011-0722-5.

Musgrove, M., and Banner, J.L., 2004, Controls on the spatial and temporal variability of vadose dripwater geochemistry: Edwards aquifer, central Texas: Geochimica et cosmochimica acta, v. 68, p. 1007–1020, doi:10.1016/j.gca.2003.08.014.

Nava-Fernandez, C., Hartland, A., Gázquez, F., Kwiecien, O., Marwan, N., Fox, B., Hellstrom, J., Pearson, A., Ward, B., French, A., Hodell, D. A., Immenhauser, A., Breitenbach, S. F. M., 2020, Pacific climate reflected in Waipuna Cave drip water hydrochemistry: Hydrology and Earth System Sciences, v. 24, p. 3361–3380, doi:10.5194/hess-24-3361-2020.

Nielsen-Gammon, J.W., Banner, J. L.,Cook, B. I., Tremaine, D. M., Wong, C.I., Mace, R. E., Gao, H., Yang, Z., Gonzalez, M. F., Hoffpauir, R., Kloesel, K., 2020, Unprecedented Drought Challenges for Texas Water Resources in a Changing Climate: What Do Researchers and Stakeholders Need to Know? Earth's Future, v. 8, p. e2020EF001552, doi:10.1029/2020EF001552.

Rohde, M.M., Albano, C. M., Huggins, X., Klausmeyer, K. R., Morton, C., Sharman, A., Zaveri, E., Saito, L., Freed, Z., Howard, J. K., Job, N., Richter, H., Toderich, K., Rodella, A., Gleeson, T., Huntington, J., Chandanpurkar, H. A., Purdy, A.

https://doi.org/10.5194/egusphere-2025-2623
Preprint. Discussion started: 2 October 2025

J., Famiglietti, J. S., Singer, M. B., Roberts, D. A., Caylor, K., Stella, J. C., 2024, Groundwater-dependent ecosystem map exposes global dryland protection needs: Nature, v. 632, p. 101–107, doi:10.1038/s41586-024-07702-8.

Schindel, G. M., 2019, Genesis of the Edwards (Balcones Fault Zone) Aquifer, in A. M. McCraw and R. E. H. West, eds., The Edwards Aquifer: The Past, Present, and Future of a Vital Water Resource: Geological Society of America, p. 9–18, https://doi.org/10.1130/2019.1215(02).

Schindel, G.M., and Gary, M., 2017, Hypogene processes in the balcones fault zone segment of the Edwards aquifer of south-central Texas, in Hypogene Karst Regions and Caves of the World, Cham, Springer International Publishing, p. 647–652, doi:10.1007/978-3-319-53348-3_41.

Smart, P.L, Friederich, H., 1987, Water movement and storage in the unsaturated zone of a maturely karstified carbonate aquifer, Mendip Hills, England." Proceedings of the Environmental Problems in Karst Terranes and Their Solutions Conference. National Water Well Association, Dublin OH. 1986. p 59-87,

Stevanović, Z., 2019, Karst waters in potable water supply: a global scale overview: Environmental Earth Sciences, v. 78, p. 1–12, doi:10.1007/s12665-019-8670-9.

Stigter, T.Y., Miller, J., Chen, J., and Re, V., 2022, Groundwater and climate change: threats and opportunities: Hydrogeology Journal, v. 31, p. 7–10, doi:10.1007/s10040-022-02554-w.

Texas Water Development Board (TWDB), 2022, 2022 State Water Plan, Water for Texas: https://www.twdb.texas.gov/waterplanning/swp/2022/docs/SWP22-Water-For-Texas.pdf (accessed April, 2025).

Texas Water Development Board (TWDB), Groundwater: https://www.twdb.texas.gov/groundwater/index.asp (accessed May, 2023).

Texas Comptroller of Public Accounts, Texas Water Tour: Groundwater: https://comptroller.texas.gov/economy/economic-data/water/2022/ground.php (accessed May, 2023).

Tooth, A.F., and Fairchild, I.J., 2003, Soil and karst aquifer hydrological controls on the geochemical evolution of speleothem-forming drip waters, Crag Cave, southwest Ireland: Journal of Hydrology, v. 273, p. 51–68, doi:10.1016/S0022-1694(02)00349-9.

Vauter, B., 2022. Map of the Natural Bridge Caverns: Natural Bridge Caverns.

Williams, P.W., 1983, The role of the subcutaneous zone in karst hydrology: Journal of Hydrology, v. 61, p. 45–67, doi:10.1016/0022-1694(83)90234-2.

Wong, C.I., Banner, J.L., and Musgrove, M., 2011, Seasonal dripwater Mg/Ca and Sr/Ca variations driven by cave ventilation: Implications for and modeling of speleothem paleoclimate records: Geochimica et Cosmochimica Acta, v. 75, p. 3514–3529, doi:10.1016/j.gca.2011.03.025.

Wong, C.I., Mahler, B.J., Musgrove, M., and Banner, J.L., 2012, Changes in sources and storage in a karst aquifer during a transition from drought to wet conditions: Journal of hydrology, v. 468-469, p. 159–172, doi:10.1016/j.jhydrol.2012.08.030.

Wu, S., Ma, D., Liu, Z., Chen, L., Chen, L., and Zhang, J., 2023, A novel approximate solution to slope rainfall infiltration: Journal of hydrology, v. 625, p. 130039, doi:10.1016/j.jhydrol.2023.130039.

https://doi.org/10.5194/egusphere-2025-2623
Preprint. Discussion started: 2 October 2025

699 Yinglan, Wang, G., Sun, W., Xue, B., and Kiem, A., 2018, Stratification response of soil water content during rainfall events
700 under different rainfall patterns: Hydrological processes, v. 32, p. 3128–3139, doi:10.1002/hyp.13250.
701
702 **Funding:** The authors thank the Kimbell School of Geosciences at Midwestern State University for financial support of this
703 study. Additional grant funding was received from AmericaView (TexasView) and the Association for Women Geoscientists
704 (AWG) - Lone Star Chapter.
705
706 **Acknowledgements:** We are grateful to the Wuest family and the Natural Bridge Caverns staff for access to the monitoring
707 site and continued care of the installed drip loggers.
708
709 **Data and Code Availability:** Logger excel data files, MATLAB and R Studio codes can be accessed at:
710 https://github.com/RNRemie/NBC_drip_loggers_2023_2024
711
712 **Conflicts of Interest:** The authors declare no conflicts of interest. The funders had no role in the design of the study; in the
713 collection, analyses, or interpretation of data; in the writing of the manuscript; or in the decision to publish the results.